NASA/TM—2013-216496

Modeling Analysis for NASA GRC Vacuum Facility 5 Upgrade

J.T. Yim and D.A. Herman
Glenn Research Center, Cleveland, Ohio

J.M. Burt
Air Force Research Laboratory, Glenn Research Center, Cleveland, Ohio

February 2013

NASA STI Program . . . in Profile

Since its founding, NASA has been dedicated to the advancement of aeronautics and space science. The NASA Scientific and Technical Information (STI) program plays a key part in helping NASA maintain this important role.

The NASA STI Program operates under the auspices of the Agency Chief Information Officer. It collects, organizes, provides for archiving, and disseminates NASA's STI. The NASA STI program provides access to the NASA Aeronautics and Space Database and its public interface, the NASA Technical Reports Server, thus providing one of the largest collections of aeronautical and space science STI in the world. Results are published in both non-NASA channels and by NASA in the NASA STI Report Series, which includes the following report types:

- TECHNICAL PUBLICATION. Reports of completed research or a major significant phase of research that present the results of NASA programs and include extensive data or theoretical analysis. Includes compilations of significant scientific and technical data and information deemed to be of continuing reference value. NASA counterpart of peer-reviewed formal professional papers but has less stringent limitations on manuscript length and extent of graphic presentations.

- TECHNICAL MEMORANDUM. Scientific and technical findings that are preliminary or of specialized interest, e.g., quick release reports, working papers, and bibliographies that contain minimal annotation. Does not contain extensive analysis.

- CONTRACTOR REPORT. Scientific and technical findings by NASA-sponsored contractors and grantees.

- CONFERENCE PUBLICATION. Collected papers from scientific and technical conferences, symposia, seminars, or other meetings sponsored or cosponsored by NASA.

- SPECIAL PUBLICATION. Scientific, technical, or historical information from NASA programs, projects, and missions, often concerned with subjects having substantial public interest.

- TECHNICAL TRANSLATION. English-language translations of foreign scientific and technical material pertinent to NASA's mission.

Specialized services also include creating custom thesauri, building customized databases, organizing and publishing research results.

For more information about the NASA STI program, see the following:

- Access the NASA STI program home page at *http://www.sti.nasa.gov*

- E-mail your question to *help@sti.nasa.gov*

- Fax your question to the NASA STI Information Desk at 443–757–5803

- Phone the NASA STI Information Desk at 443–757–5802

- Write to:
  STI Information Desk
  NASA Center for AeroSpace Information
  7115 Standard Drive
  Hanover, MD 21076–1320

NASA/TM—2013-216496

Modeling Analysis for NASA GRC Vacuum Facility 5 Upgrade

J.T. Yim and D.A. Herman
Glenn Research Center, Cleveland, Ohio

J.M. Burt
Air Force Research Laboratory, Glenn Research Center, Cleveland, Ohio

National Aeronautics and
Space Administration

Glenn Research Center
Cleveland, Ohio 44135

February 2013

Level of Review: This material has been technically reviewed by technical management.

Available from

NASA Center for Aerospace Information
7115 Standard Drive
Hanover, MD 21076–1320

National Technical Information Service
5301 Shawnee Road
Alexandria, VA 22312

Available electronically at http://www.sti.nasa.gov

Abstract

A model of the VF5 test facility at NASA Glenn Research Center was developed using the direct simulation Monte Carlo Hypersonic Aerothermodynamics Particle (HAP) code. The model results were compared to several cold flow and thruster hot fire cases. The main uncertainty in the model is the determination of the effective sticking coefficient—which sets the pumping effectiveness of the cryopanels and oil diffusion pumps including baffle transmission. An effective sticking coefficient of 0.25 was found to provide generally good agreement with the experimental chamber pressure data. The model, which assumes a cold diffuse inflow, also fared satisfactorily in predicting the pressure distribution during thruster operation. The model was used to assess other chamber configurations to improve the local effective pumping speed near the thruster. A new configuration of the existing cryopumps is found to show more than 2× improvement over the current baseline configuration.

1 Introduction

Vacuum Facility 5 (VF5) at NASA Glenn Research Center is one of the world's premier electric propulsion (EP) test facilities. The main chamber is 4.6 m (15 ft) in diameter and nearly 18 m (60 ft) long. Six cryopumps and twenty oil diffusion pumps (ODP) can provide a base pressure on the order of 1×10^{-7} torr and a theoretical maximum pumping speed over 3.5 million L/s on air. However, due to the present baseline configuration of the chamber, the actual local pumping speed can be far lower, particularly at the end of the chamber away from the cryopumps. The conductance losses through the chamber are in part responsible for this [1]. As NASA moves toward higher power EP systems, the need for facilities to provide adequate ground testing capabilities is required. A sufficiently low background pressure is necessary for proper characterization of thruster performance, plume properties, and lifetime [2–4]. Thus, an effort to improve the effective pumping speed of VF5 is underway. As part of that effort, the capabilities of VF5 are modeled to provide understanding of facility pumping and to assess new potential configurations. Both cold flow and thruster hot fire test data are collected to provide comparisons for model validation. A description of the model, the testing, and results and comparisons of both are discussed below.

2 Model and Test Description

The Hypersonic Aerothermodynamics Particle (HAP) code was used to perform 3D Direct Simulation Monte Carlo (DSMC) simulations of facility pressure distributions for VF5 [5]. The rarified environment of an operating vacuum chamber makes DSMC an ideal approach for these simulations. The DSMC method is a particle-based gas flow simulation technique which is derived from principles of kinetic theory, and is the most mature and widely used technique for rarefied flow simulation. In a DSMC calculation, a large population of simulated particles is tracked through the computational domain, with a combination of deterministic particle movement routines and probabilistic binary collision routines, in order to simulate underlying physics in the governing Boltzmann equation. The HAP code is a general Cartesian implementation of DSMC, with features including dynamic grid adaptation; shared memory parallelization; and options to import externally defined surface geometries or to automatically generate triangulated surfaces based on analytical geometry definitions.

For the VF5 models, the chamber geometry—namely the outer shell of the main chamber and bell jar—is analytically defined within the code through spherical and cylindrical shells. Also included are the graphite shielding panels placed approximately midway along the chamber length to protect the cryopanels from direct plume impingement. VF5 contains six large cryopanels and twenty 32" diameter ODPs. A diagram of the current baseline configuration is provided in Figure 1.

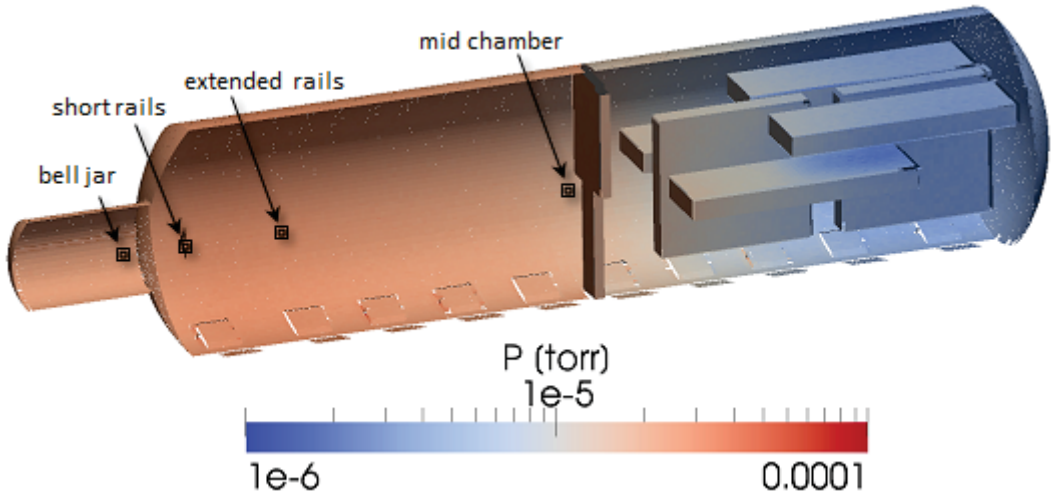

Figure 1. The baseline configuration of VF5 with four markers indicating approximate gas source locations. The pressure distribution coloring is based on a short rails source location and 60 mg/s xenon gas flow.

The two vertical cryopanels along the chamber centerline are 2.8 m × 3.0 m × 0.5 m in size and they pump along their left and right vertical surfaces. The four horizontal cryopanels are 0.4 m × 4.6 m × 1.4 m in size and pump along their top and bottom horizontal surfaces. The ODPs are modeled to have a square pumping surface rather than circular for simplicity; the surface area is kept the same. No other details of the vacuum facility geometry are explicitly modeled. The symmetrical nature of the vacuum chamber across the vertical plane along the chamber centerline is utilized to reduce the simulated volume in half.

The gas source is modeled as an annulus with a uniformly distributed inflow number flux to simulate the flow exiting a Hall thruster discharge channel. The inflow number flux is calculated to achieve the desired mass flow rate. The rest of the thruster and support structure geometry are not modeled in these simulations. The inflow gas is modeled as a diffuse inflow at room temperature, which is appropriate for cold gas flow conditions. Thruster hot fire is not directly modeled as Hall thruster propellant particle exit velocities are high enough to require a prohibitively small time step to resolve their motion and physics. Results presented below, however, will show that the cold diffuse flow inflow conditions still approximate hot fire conditions to a fair degree. Other research work has shown only minor differences noted for adding electrostatic fields and/or charge exchange physics to DSMC flow simulations [6].

The model of VF5 was correlated to experimental pressure data to assess confidence in the simulation results. Several different available data cases were used to check the validity of the model. They are listed in Table 1. Four xenon gas source locations were used for the various tests and their approximate positions are shown in Figure 1. The "short rails" location placed the source, typically a thruster, approximately at the end cap / main chamber interface axial location. The "extended rails" location is approximately 1.5 m further into the main chamber. The "mid chamber reverse" placed the source just in front of the vertical shielding panels facing upstream back towards the bell jar. The pressure color contour distribution in Figure 1 is based on 60 mg/s xenon gas flow from the short rails location. Unless explicitly stated otherwise, all gas flow rates, pressures, and pumping speeds reported in this document are for xenon gas.

The measured chamber pressure data are obtained using Granville-Phillips ion gauges and have been corrected for xenon gas, which is used for all tests considered here. The ion gauge locations are largely in the same locations for all tests and reported in Table 2. For the azimuthal locations,

Table 1. Test data sources

#	Date	Source	Source location	Active pumps
1	May 2011	Cold flow	Bell jar & mid chamber	Cryos only
2	Oct 2011	Cold flow	Short rails	ODPs only
3	Oct 2011	Cold flow	Short rails	Cryos + ODPs
4	Nov 2011	Cold flow	Short rails	Cryos + ODPs
5	Nov 2011	Hot fire	Short rails	Cryos + ODPs
6	Jan 2012	Hot fire	Mid chamber reverse	Cryos + ODPs
7	Apr 2012	Hot fire	Extended rails	Cryos only

Table 2. Ion gauge locations

Gauge	Uncertainty	Radial	Azimuthal	Axial
G-P 347 Stabil-Ion Module	±25%	Along main chamber wall	∼8:00	∼1 ft from end cap
G-P 390 Micro-Ion Module	±16%	Along main chamber wall	∼8:00	∼1 ft from end cap
G-P 390 Micro-Ion Module	±16%	Along main chamber wall	∼4:00	∼26 ft from end cap
G-P 390 Micro-Ion Module	±16%	Along main chamber wall	∼4:00	∼46 ft from end cap
G-P 370 Stabil-Ion Gauge	±5%	∼0.75 m from centerline	∼4:00	Along thruster exit plane

noon is along the vertical and the clockwise direction is based on looking into the chamber from the bell jar end. The 95% confidence intervals of the chamber pressure reading uncertainties for each ion gauge are also provided in Table 2. They are based on the accuracy and repeatability values reported by the manufacturer. Error bars for the chamber pressure measurements in the plots within Section 3 are set to these 95% confidence level values.

The primary unknown variable in these simulations is the sticking coefficient—the fraction of incident particles that are effectively pumped through cryocondensation, cryosorption, or cryotrapping. The sticking coefficients of gases on a bare cryosurface have been found to lie generally within a range of 0.6 – 1.0 depending on the gas and surface temperature [7]. However, the VF5 cryopumps have liquid nitrogen-cooled chevron baffles in front of the cryosurfaces. The transmission probabilities through these baffles—which were provided to be 0.30 to 0.35—are accounted for through a modified effective sticking coefficient. A series of computational runs was performed to assess the sensitivity of the modeling results to the applied effective sticking coefficient. The model was set up to correspond to tests #3 and 4 in Table 1. The effective sticking coefficient was varied from 0.15 to 0.40 in increments of 0.05. The pressure was assessed at four locations corresponding to the bottom four gauges listed in Table 2. The averaged measured pressures with their corresponding uncertainty are plotted as shaded bands in Figure 2. The model results are plotted as symbols. For the pressure near the chamber walls, an effective sticking coefficient of 0.20 to 0.25 was found to provide the best guess fit. The near thruster pressure data required a sticking coefficient closer to 0.40. As a general compromise, with some emphasis on the chamber wall locations where most of the test data is and will be measured, an effective sticking coefficient of 0.25 was chosen. This is comparable to other published cryopumping simulation work which has found values around 0.3 – 0.4 for the effective coefficient to provide a good fit to their data [8]. An effective sticking coefficient of 0.25 is used for all results presented below.

Some of the results are presented in terms of pumping speed instead of pressure. The pumping speed is easily calculated from

$$PS = \frac{(\dot{m}\ \text{mg/s})(22.4\ \text{L-atm/mol})(760\ \text{torr/atm})}{(1000\ \text{mg/g})(M\ \text{g/mol})(P - P_{base}\ \text{torr})} \tag{1}$$

where $\dot{m}$ is the mass flow rate, M is the molecular weight of the gas, and P_{base} is the base pressure measured when there is no gas inflow. The model assumes a perfectly leak tight vessel with no

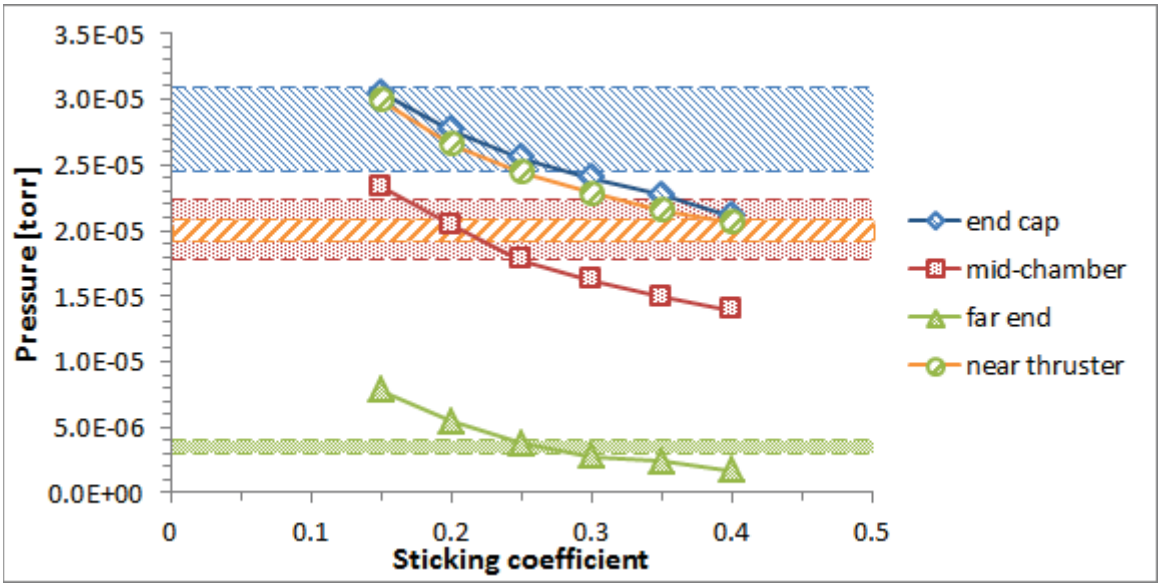

Figure 2. The effect of the sticking coefficient on modeled chamber pressures at four locations. The shaded bars correspond to the 95% confidence interval of the measured test data at those four locations. The symbols plot the model results.

presence of non-condensable species such as helium, therefore P_{base} would theoretically be zero for the model. Since the pressure in the chamber will vary with location, the pumping speed too will vary throughout the chamber.

3 Results and Discussion

The VF5 model is run for several cases corresponding to different thruster and chamber configurations. For all cases, the location and orientation of the cryopumps and ODPs are the same. A set of tests were run that operated: 1) cryos only, 2) ODPs only, and 3) all pumps in the chamber. The effect of the pumping scheme is evaluated with the model. Results are presented in Figure 3. The model shows a fair approximation to the pressure data collected along the chamber wall. The model results for the ODP-only case does not capture the drop in pressure at the far end of the channel, however, the overall magnitude of the pressure tracks with the recorded data, particularly near the thruster, which is the location of most interest. Different xenon gas flow rates were also examined. Testing included adjusting the inflow rate of xenon cold gas inflow from 20 to 107 mg/s with all of the pumps operating. Models were run at 20, 60, and 100 mg/s and the results are compared in Figure 4. Again, the magnitude of pressure change is well captured by the model.

The model was also compared to pressure data obtained during thruster hot fire testing. The model assumes a diffuse cold gas inflow, as simulating the high velocity plume particles requires prohibitively small time steps. Test #5 in Table 1 corresponds to NASA-457Mv2 Hall thruster performance testing at flow rates ranging from 18.5 to 92.4 mg/s [9]. Pressure data were collected from a screen-shielded Stabil-ion gauge located 0.75 m from the thruster centerline along the thruster exit plane. Similar data were collected from cold flow test #4 with the same thruster, chamber, and ion gauge configuration. The results from the two tests and the corresponding cold flow model results are shown in Figure 5.

Two other thruster hot fire cases are examined. Both operate the thruster at different locations than the standard location on the short rails. The thruster is placed on an extended set of rails further into the main chamber for one test, while the other places the thruster near mid-chamber

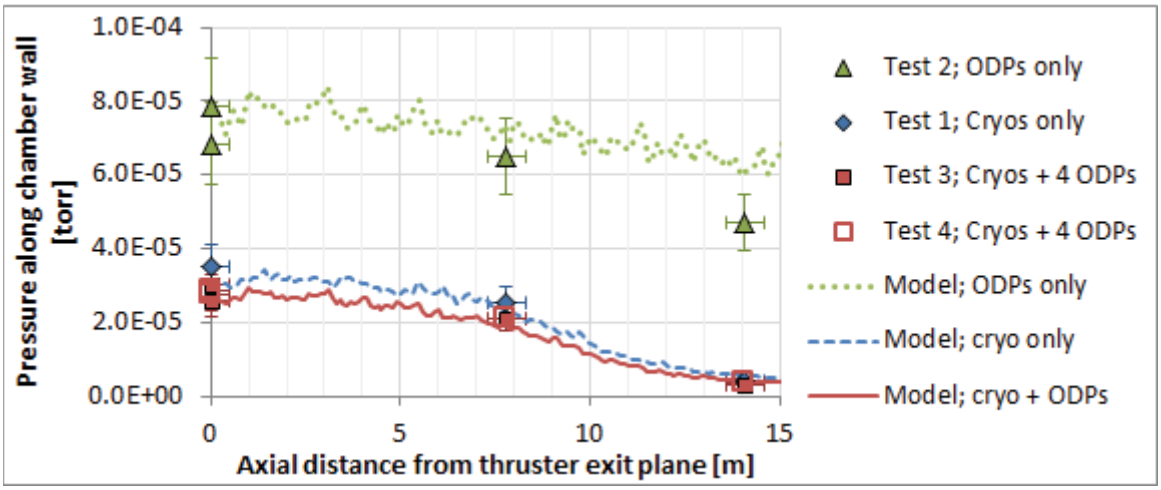

Figure 3. Comparison of model and test chamber pressure results for different pumping operations in VF5.

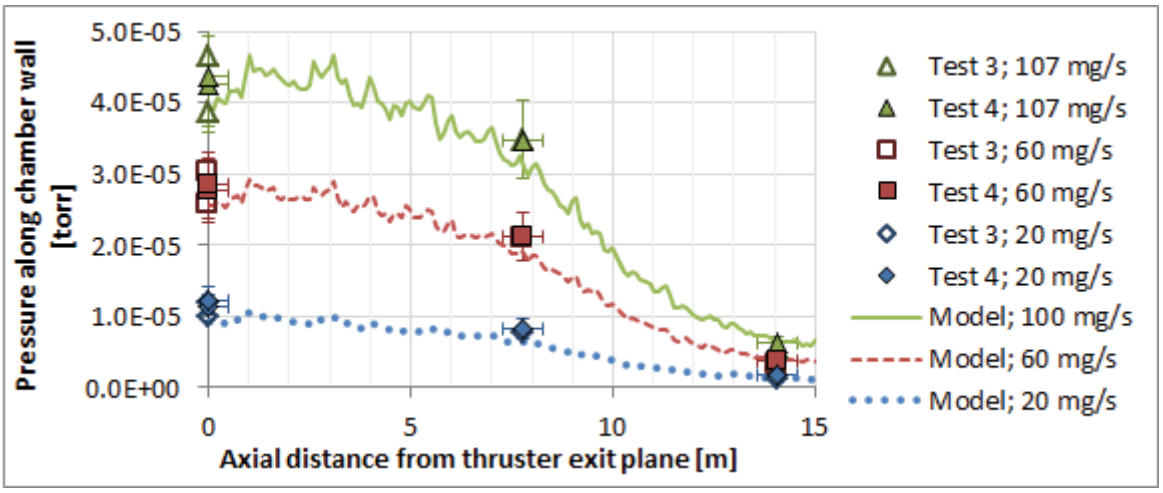

Figure 4. Comparison of model and test chamber pressure results for different flow rates in VF5.

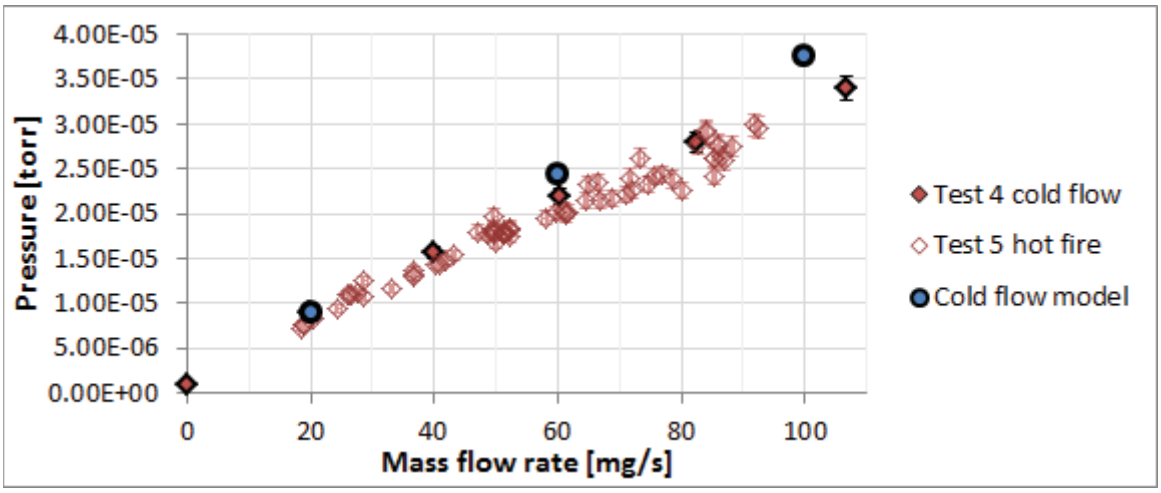

Figure 5. Comparison of chamber pressure results 0.75 m from thruster centerline for cold flow test, hot fire test, and cold flow model.

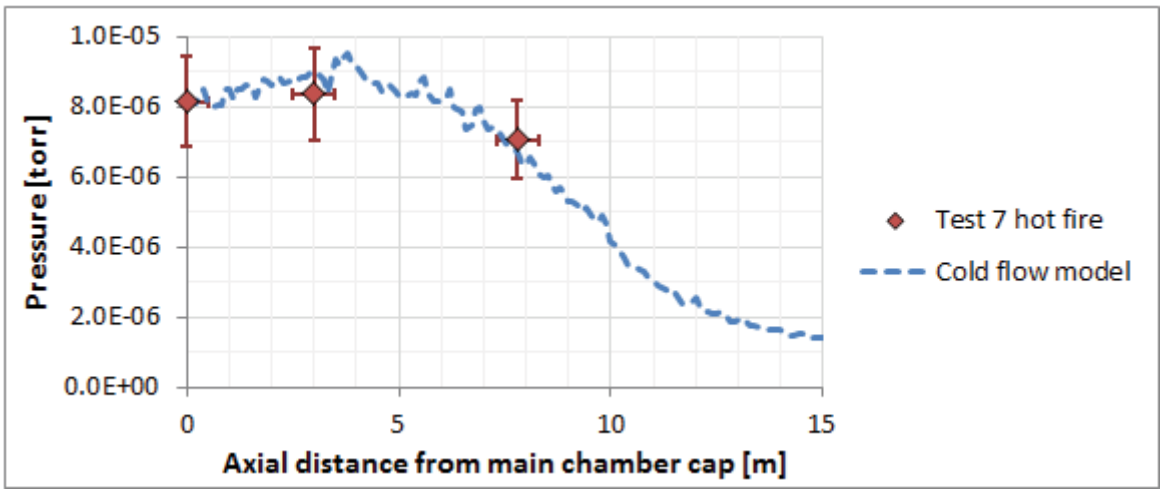

Figure 6. Comparison of chamber pressure along chamber walls for the extended rails thruster location hot fire test.

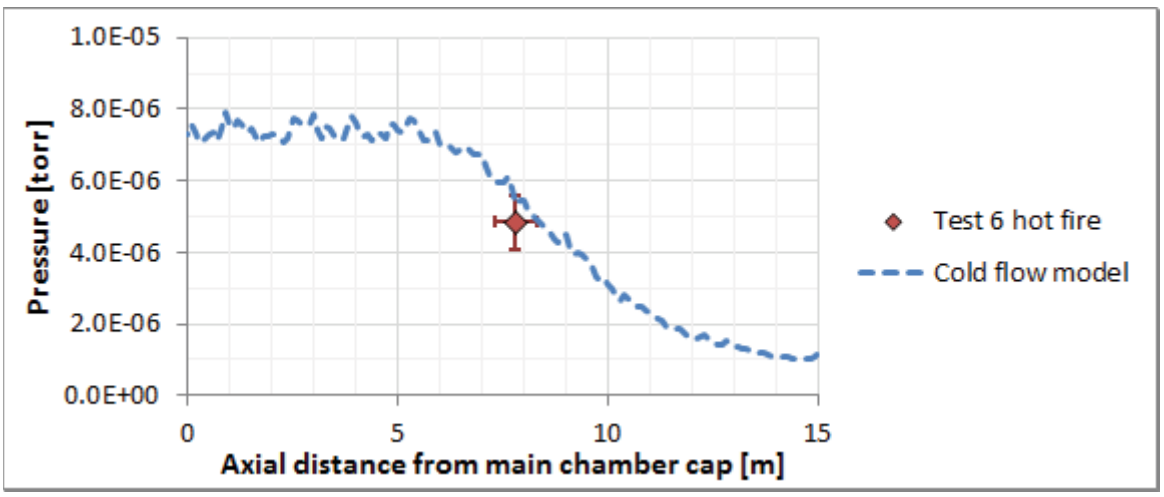

Figure 7. Comparison of chamber pressure along chamber walls for the mid chamber reverse thruster location hot fire test.

and points the thruster back towards the bell jar end. The model was run for both of those cases. The comparison for the extended rails configuration is shown in Figure 6 and the mid chamber reversed configuration is shown in Figure 7.

The test cases described above provide a confidence in the ability of the model to predict the chamber pressure for the baseline configuration of VF5. The model was utilized to assess the pumping speed of alternate VF5 configurations. The other configurations included moving the existing panels as well as adding new ones. The initial set of configurations examined is presented in Figure 8. It is seen that the presence of cryopanels along the length of the chamber significantly reduces the pressure in the upstream regions of the chamber near the thruster, as compared to the baseline configuration. This is due to reducing conductance losses before the gas reaches a pumping surface [1].

Ultimately, a configuration relocating all of the existing cryopanels was chosen based on pumping effectiveness, cost, backsputter rate, and other facility considerations. The new proposed chamber configuration moves the long horizontal panels upstream closer to the bell jar as shown in Figure 8(d). The two vertical panels will also be moved parallel to each other at the far end of

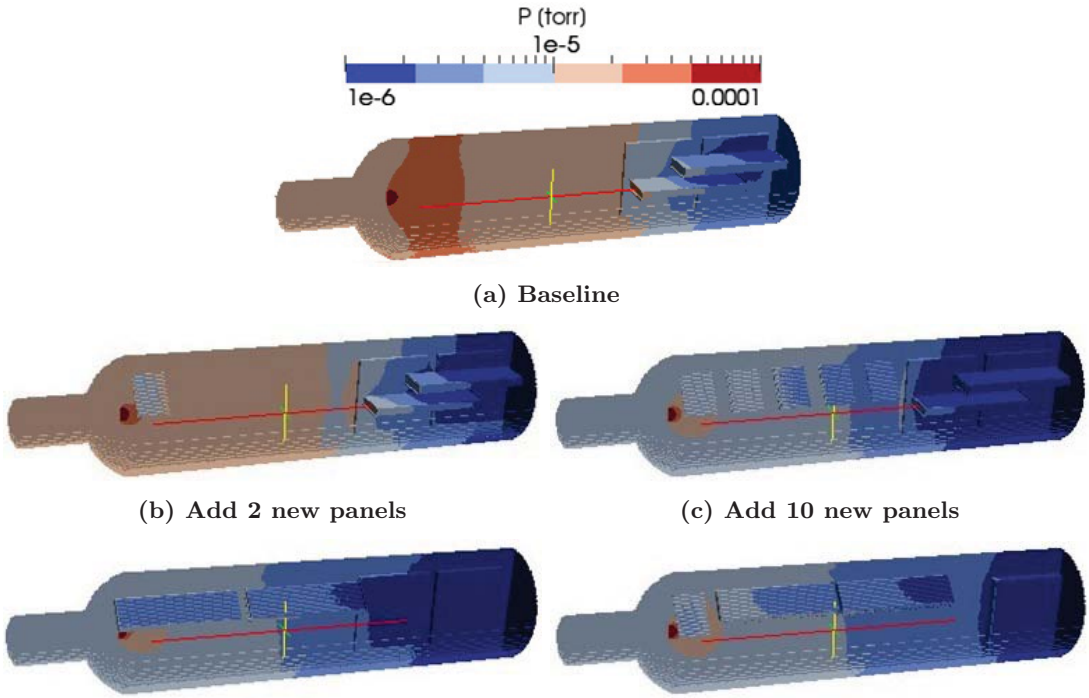

(a) Baseline

(b) Add 2 new panels

(c) Add 10 new panels

(d) Move horizontal panels

(e) Move all existing panels, add 2 new panels

Figure 8. Initial set of chamber configurations examined.

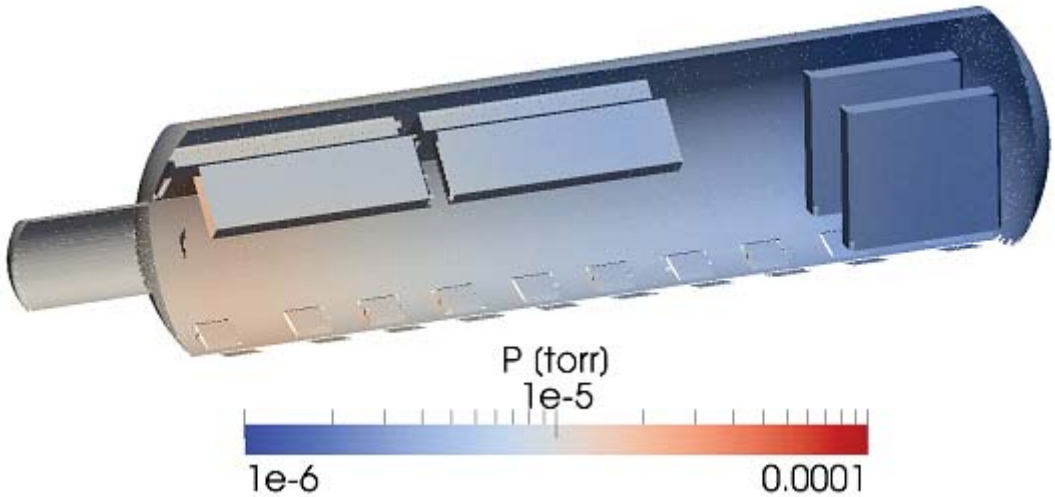

Figure 9. The new proposed configuration of VF5 which rearranges all existing cryopanels. The pressure distribution coloring is based on a short rails source location and 60 mg/s xenon gas flow.

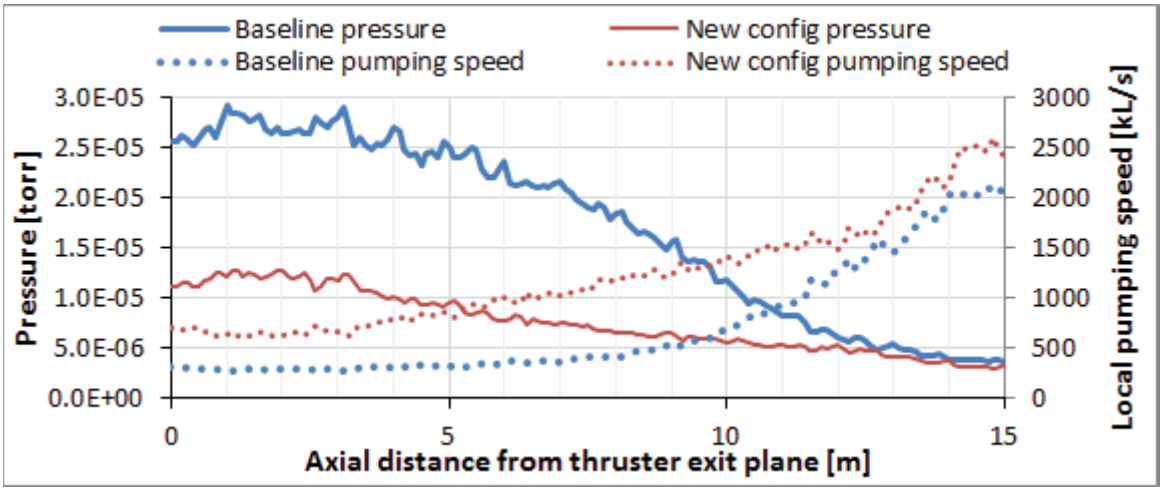

(a) Axial distribution of pressure and local pumping speed along chamber wall

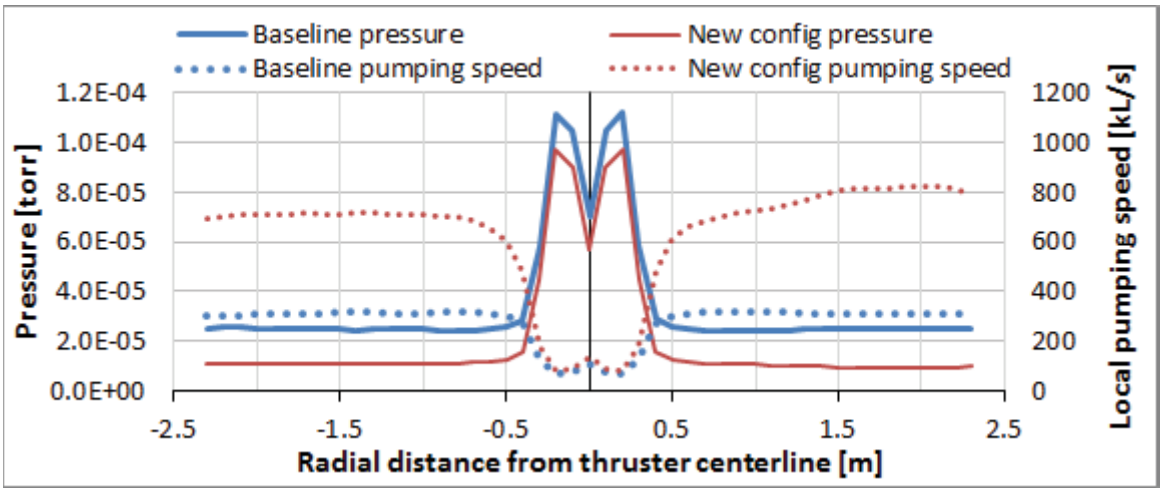

(b) Radial distribution of pressure and local pumping speed along thruster exit plane

Figure 10. Comparisons of pressure and local pumping speed distributions between baseline and new proposed chamber configurations for 60 mg/s xenon flow at the short rails location.

the chamber as configured in Figure 8(e). A model of the new configuration was developed and is shown in Figure 9. Both Figure 9 and Figure 1, of the baseline configuration, show a pressure distribution based on 60 mg/s of xenon flow from a thruster at the "short rails" location. A closer look at the pressure distribution is shown in Figure 10. The axial distribution of the pressure along the chamber wall again shows a marked reduction in the upstream pressure towards the thruster location while the downstream pressure near the far end of the chamber is similar as before. The radial pressure distribution along the thruster exit plane vertical axis also shows improvement over the current baseline. The pumping speed is calculated for both configurations based on the pressure 0.75 m from the thruster centerline along the thruster exit plane and shown in Figure 11. More than two times improvement, from 320 kL/s to 700 kL/s, is seen in the modeling results for a 60 mg/s flow rate. The pumping speeds calculated from pressure measurements at the same location during thruster hot fire tests are also shown in the figure.

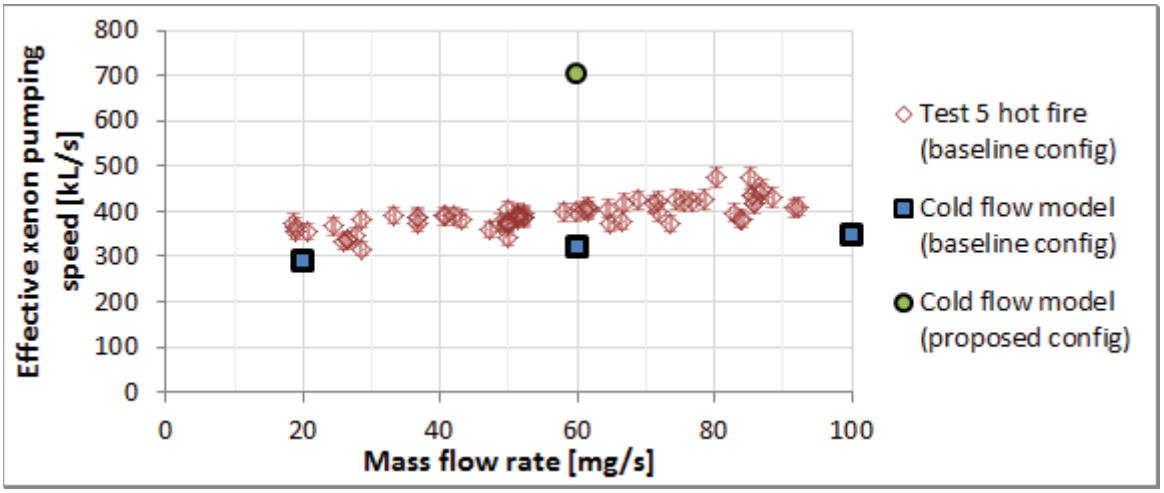

Figure 11. Comparison of calculated xenon pumping speeds 0.75 m from thruster centerline in exit plane.

4 Conclusion

A model of VF5 was developed and run using the HAP DSMC code. The baseline cryopanel configuration of VF5 was examined across several different source and pumping cases to assess the validity of the model as compared to measured test data. VF5 was operated with different pumps activated, different gas inflow rates, and different thruster locations. The model captured the pressure changes along the length of the chamber and compared well with test results. The main source of uncertainty in the modeling results was the estimation of the effective sticking coefficient used to model the effects of the transmission probability through the baffles in front of the pumping surfaces as well as the sticking probability of the gas particles to be pumped away after they reach the pumping surface. A coefficient of 0.25 was found to achieve an acceptable comparison to the measured test data for the cases examined. One other possible significant contributor to model uncertainty is the approximate geometry of the chamber and its contents. A more detailed geometrical description of the chamber, as perhaps represented in a high fidelity CAD model, would help further reduce uncertainty in the model results.

In addition to the present baseline configuration of VF5, several new variants were examined to assess potential improvements in pumping speed throughout the chamber. These options included moving the current existing cryopanels as well as including additional new panels. Ultimately, a new configuration that rearranges the existing panels was chosen based on a variety of factors. The new configuration is expected to provide more than 2× the pumping speed near the thruster than the present baseline setup.

References

1. Dankanich, J. W., Swiatek, M. W., and Yim, J. T., "A Step Towards Electric Propulsion Testing Standards: Pressure Measurements and Effective Pumping Speeds," *48th AIAA/ASME/SAE/ASEE Joint Propulsion Conference & Exhibit*, 2012, AIAA-2012-3737.

2. Randolph, T., Kim, V., Kaufman, H., Kozubsky, K., Zhurin, V., and Day, M., "Facility Effects on Stationary Plasma Thruster Testing," *23rd International Electric Propulsion Conference*, 1993, IEPC 93-93.

3. Byers, D. and Dankanich, J. W., "A Review of Facility Effects on Hall Effect Thrusters," *31st International Electric Propulsion Conference*, 2009, IEPC-2009-076.

4. Diamant, K. D., Spektor, R., Beiting, E. J., Young, J. A., and Curtiss, T. J., "The Effects of Background Pressure on Hall Thruster Operation," *48th AIAA/ASME/SAE/ASEE Joint Propulsion Conference and Exhibit*, 2012, AIAA 2012-3735.

5. Burt, J. M., Josyula, E., and Boyd, I. D., "Novel Cartesian Implementation of the Direct Simulation Monte Carlo Method," *Journal of Thermophysics and Heat Transfer*, Vol. 26, No. 2, 2012.

6. Boyd, I. D., Sun, Q., and Cai, C., "Particle Simulation of Hall Thruster Plumes in the 12V Vacuum Chamber," *29th International Electric Propulsion Conference*, 2005, IEPC-2005-138.

7. Ketsdever, A. D., "Design Considerations for Cryogenic Pumping Arrays in Spacecraft-Thruster Interaction Facilities," *Journal of Spacecraft and Rockets*, Vol. 38, No. 3, 2001.

8. Walker, M. L. R., Gallimore, A. D., Boyd, I. D., and Cai, C., "Vacuum Chamber Pressure Maps of a Hall Thruster Cold-Flow Expansion," *Journal of Propulsion and Power*, Vol. 20, No. 6, 2004.

9. Soulas, G. C., Haag, T. W., Herman, D. A., Huang, W., Kamhawi, H., and Shastry, R., "Performance Test Results of the NASA-457M v2 Hall Thruster," *48th AIAA/ASME/SAE/ASEE Joint Propulsion Conference and Exhibit*, 2012, AIAA 2012-3940.